Surface Properties of Surfactant-Free Oil Droplets Dispersed in Water Studied by Confocal Fluorescence Microscopy

Toshio Sakai,[†,§] Yoshihiro Takeda,[†] Fumitaka Mafuné,[‡,⊥] and Tamotsu Kondow*[,‡]

East Tokyo Laboratory, Genesis Research Institute, Inc., 717-86 Futamata, Ichikawa, Chiba 272-0001, Japan, and Cluster Research Laboratory, Toyota Technological Institute, 717-86 Futamata, Ichikawa, Chiba 272-0001, Japan

Received: September 30, 2003; In Final Form: March 11, 2004

The fluorescence spectrum of dye molecules, 4-(dicyanomethylene)-2-methyl-6-(*p*-dimethylaminostyryl)-4*H*-pyron (DCM), dissolved in surfactant-free *n*-decane droplets (average diameters of ∼300 and ∼2000 nm) dispersed in water was measured by a confocal microscope. The fluorescence spectra for 300- and 2000-nm droplets are found to exhibit a peak at 640 and 625 nm, respectively, and the peak red shifts with a decrease in the droplet diameter (solvatochromic shift of DCM molecules). It is concluded that (1) DCM molecules are located in a polar surface region of *n*-decane droplets and (2) the polarity increases with decreasing the droplet diameter.

Introduction

An interface between two liquids has been investigated intensively because the interface influences most significantly the fundamental properties of fine liquid particles; needless to say, these particles always play a decisive role in colloidal and biological processes, material separation, etc. In this relation, surface-sensitive spectroscopic techniques have been developed to investigate the properties of the interface in a nondestructive manner.[1−8] Confocal fluorescence microscopy (CFM) is one of such techniques developed recently, which enables us to conduct highly sensitive measurements of the interface.[9−12] With a confocal setup, the probe volume of a confocal microscope less than a femtoliter can be attained so that the background noise limiting the sensitivity of the measurements is greatly reduced.[12] The depth of the probe volume is in the range of several hundred nanometers, which would be too thick to monitor the behavior of molecules on the very surface of the interface.[13] In a particular case, the CFM technique provides useful information on the interface. For instance, Zheng et al. have demonstrated the utility of CFM under a limited depth resolution in the studies of insoluble chromophores as well as surface-active soluble chromophores in air−water and oil−water interfaces.[14−16] On the other hand, the extremely small probe volume of CFM facilitates detection and identification of nanometer-sized droplets dispersed in a liquid.[17,18] Actually, we have observed dye-labeled surfactant-free *n*-decane droplets dispersed in water by using CFM and have revealed that dye molecules in a given droplet permeate through the *n*-decane−water interface at a rate that depends critically on the droplet diameter.[17]

In the present work, we employed CFM for the measurements of the fluorescence spectra of 4-(dicyanomethylene)-2-methyl-6-(*p*-dimethylaminostyryl)-4*H*-pyron (DCM) dissolved in surfactant-free *n*-decane droplets dispersed in water and derived the orientation polarizability of the interface between the *n*-decane droplets and water. The dye molecule, DCM, shows several advantages in the studies of the polarizability of the interface. A solvatochromic shift caused by twisted intramolecular charge transfer (TICT) in the excited state,[19−27] for example, gives direct information on the polarity environment of the *n*-decane droplets in water. A fluorescence peak of DCM appears at ∼620 nm with a quantum yield of ∼0.35, ∼0.40, and ∼0.55 in anionic (sodium dodecyl sulfate (SDS), etc.), cationic (cethyl trimethylammonium bromide (CTAB), etc.), and neutral micelle solutions (Triton X-100, etc.), respectively; DCM molecules are present in a highly polar region of the micelles but not in the hydrocarbon core of them.[28] In a solution of Triton X-100, DCM molecules are fully enclosed inside the palisade layer, so that they do not interact directly with the fast-moving bulk water molecules. On the other hand, a major portion of DCM molecules in the thin Stern layer of CTAB and SDS solutions are exposed to bulk water and experience fast solvation dynamics. It should be pointed out that when di(ethylhexy)-sulfosuccinate (AOT) and water with a 1:20 molar ratio are mixed with a solution of DCM in *n*-heptane for preparing a water-in-*n*-heptane microemulsion stabilized by AOT, the DCM molecules migrate partly from the *n*-heptane to the water pool of the microemulsion thus prepared.[29] As described in the following sections, the present system, together with CFM having a prove volume even with a limited depth resolution, facilitates an exclusive detection of DCM in the *n*-decane−water interface of droplets.

A simplified model system should be introduced so as to manifest the essential features that the *n*-decane droplet itself owns. In this regard, surfactant-free *n*-decane droplets dispersed in water are one of the most adequate systems for scrutiny, because the emulsion is free of surfactants which would introduce irresolvable complexities in understanding the behavior of the droplets.

* Author to whom correspondence should be addressed. Phone:+81−47−320−5911. Fax: +81-47-327-8031. E-mail: kondow@clusterlab.jp.

† Genesis Research Institute, Inc.

§ Present address: Department of Chemical and Biological Engineering, University at Buffalo, The State University of New York, Buffalo, NY 14260-4200.

‡ Toyota Technological Institute.

⊥ Present address: Department of Basic Science, School of Arts and Sciences, The University of Tokyo, Komaba, Meguro, Tokyo 153-8902, Japan.

10.1021/jp036931p CCC: $27.50
Published on Web 04/23/2004

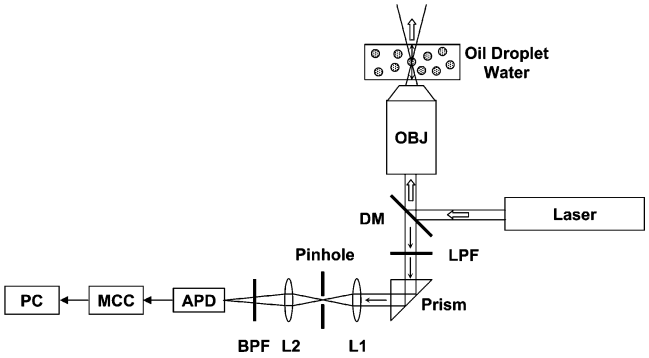

Figure 1. Schematic diagram of the experimental setup for the observation of *n*-decane droplets in water with a confocal fluorescence microscope. DM represents a dichroic mirror (DM505), LPF a long-pass filter, and L1and L2 convex lenses. The sample is placed right above an objective lens, OBJ. BPF, APD, MCC, and PC represent a band-pass filter, an avalanche photodiode, a multichannel counter, and a computer, respectively.

Experimental Section

Materials and Sample Preparation. A *n*-decane-in-water emulsion was prepared by mixing *n*-decane (GR grade, Tokyo Kasei Co., Ltd.) dissolving 1×10^{-5} mol L^{-1} of 4-(dicyanomethylene)-2-methyl-6-(*p*-dimethylaminostyryl)-4*H*-pyron (DCM; laser grade, Exciton, Inc.) with deionized water (electric conductivity of 5.58 μS cm^{-1}, Ohtsuka Pharmacy Co., Ltd.), using an ultrasonic cleaner (FU-10C, 60 W, 28 kHz, Tokyo Garasu Kikai Co., Ltd.). The concentration of *n*-decane in the water was 5×10^{-4} mol L^{-1}, and hence, the concentration of DCM in the emulsion turns out to be $\sim 1 \times 10^{-9}$ mol L^{-1}. The average diameters of virgin *n*-decane droplets and those at 2 h and at 1 day after the preparation were found to be ~50, ~300, and ~2000 nm, respectively, which were measured by the dynamic light scattering method.[17,18] In surfactant-free oil droplets dispersed in water, three metastable regions at ~50, ~300, and ~2000 nm in diameter have been generally observed.[17,18] In the *n*-decane-in-water emulsion,[18] droplets with an average diameter of ~50 nm are initially formed and remain intact for about half an hour, then the diameter jumps up to an average of ~300 nm. These 300-nm droplets are sustained for several hours until the next metastable droplets with an average diameter of ~2000 nm emerge. An effect of buoyancy of *n*-decane droplets in water caused by the density difference was not taken into account in our experiment, because the total amount of DCM molecules in the *n*-decane-in-water emulsion was conserved throughout the measurement as confirmed by observing the number and the height of the spike-like fluorescence signals.

Fluorescence Spectroscopy of DCM in Droplets. Fluorescence emitted from DCM molecules in individual droplets was focused in a confocal fluorescence microscope (IX70, OLYMPUS) and detected by an avalanche photodiode (see Figure 1). A sample solution maintained at 23 ± 1 °C was placed right above the objective lens (LUMPlan FI 100 × W, OLYMPUS), which has a numerical aperture of 1.00. An argon ion laser (Model 177G Laser System; Spectra-Physics, Co.) was used to excite DCM molecules in *n*-decane droplets at the wavelengths of 488 and 514 nm. The output wavelength of the argon ion laser was so chosen that Raman scattering light by water does not interfere with the detection of the fluorescence signals; the output wavelengths of 514 and 488 nm were selected for the detection of 520−610-nm fluorescence signals and that of 610−680-nm fluorescence signals, respectively. Raman scattering light by *n*-decane droplets was not observed in the wavelengths where the Raman scattering light should be observed, probably because the *n*-decane droplets have a volume fraction of only ~1/10000 with respect to water. Fluorescence signals from DCM molecules in individual droplets passing through the focal volume of the laser beam were collected by the same objective lens provided for focusing the excitation laser. Scattered laser light by the droplets was rejected by a long-pass filter (>515 nm). The fluorescence spectra were measured by using band-pass filters having the pass ranges of 520 ± 10, 580 ± 15, 610 ± 10, and 670 ± 20 nm, respectively. The pass wavelength of each filter was changed by adjusting the incident angle of the fluorescence with respect to the filter surface. The fluorescence was detected by an avalanche photodiode with a quantum efficiency of ~70%. The fluorescence signal was processed and registered in a multichannel counter (SR430, Stanford Research Systems) with the gate time of 10.4 ms, which was determined on the basis of the characteristic time scale of the Brownian motion of *n*-decane droplets in water. In the confocal configuration, a pinhole 50 μm in diameter was located at the conjugated position in front of the photodiode. The fluorescence was so focused at the pinhole that the fluorescence signals were maximized while undesired signals were minimized through defocusing at the pinhole. The fluorescence intensity is expressed as the counts of fluorescence photon bursts accumulated for 104 s. The fluorescence intensity measured at the laser wavelength of 514 nm is smaller by a factor of 1.98 than those at 488 nm due to the different absorbances of DCM at the two wavelengths, 488 and 514 nm. The normalization factor, 1.98, was determined by comparison of the two fluorescence intensities measured at the excitation wavelengths of 488 and 514 nm. In addition, the different transmittances of the band-path filters employed were taken into account for the signal normalization.

Fluorescence Spectroscopy of DCM in the Flat *n*-Decane−Water Interface. The fluorescence spectrum of DCM at a flat *n*-decane−water interface was obtained similarly by the procedure described in the previous section. A sample liquid was prepared by casting *n*-decane-dissolving DCM gently on water. The sample liquid thus prepared was placed right above the objective lens. The excitation laser was pinpointed at the *n*-decane−water interface. Fluorescence spectra were measured by a monochromator (MC-10N, RITSU OYO KOGAKU CO. Ltd.) in the wavelength range from 700 to 520 nm with a 5-nm interval, where the concentration of DCM in *n*-decane was changed from 10^{-10} to 10^{-5} mol L^{-1}.

Fluorescence Spectroscopy of DCM in Solution. The fluorescence spectrum of DCM in *n*-decane was measured by a fluorescence spectrometer (RF-5300PC SPECTROFLUOROPHOTOMETER, SHIMADZU) at the excitation wavelength of 488 nm. The fluorescence wavelength was scanned repeatedly from 800 to 400 nm. The cell maintained at 25 ± 0.2 °C was sealed during the measurements to avoid vaporization. The concentration of DCM in *n*-decane was varied in the range of $\sim 1 \times 10^{-7}$ to $\sim 1 \times 10^{-3}$ mol L^{-1}.

Depth Resolution of the Confocal Fluorescence Microscope. To estimate the depth resolution of the confocal fluorescence microscopy, a 625-nm fluorescence of DCM from a *n*-decane−water interface was observed with changing the focusing position along the direction perpendicular to the interface at the DCM concentration of 1×10^{-5} mol L^{-1} (see Figure 2). The fluorescence wavelength of 625 nm was chosen because the fluorescence spectrum gives the peak at ~625 nm, whereas fluorescence from liquids of *n*-decane and water is negligibly small at 625 nm.

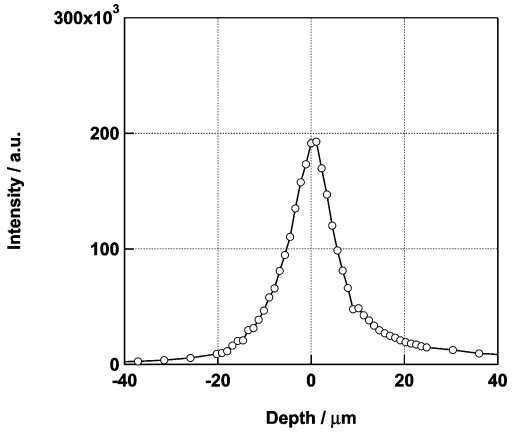

Figure 2. Depth resolution of the confocal fluorescence microscope in this present setup. The numerical aperture of the objective is 1.00. The position with the maximum intensity at the interface is set at 0 in the abscissa, of which intensity is set to be unity. The plus and minus signs represent a position in a *n*-decane liquid and a liquid water, respectively, while the interface is located at zero. The intensity of 625-nm fluorescence was monitored; the 625-nm fluorescence originates from DCM molecules in the vicinity of the interface. The concentration of DCM in *n*-decane was 1×10^{-5} mol L^{-1}.

In a confocal fluorescence microscope, the focal region is effectively confined in an elongated cylinder with a radius of ω and a height of $2d_z$. If an oil−water interface is located at the exact symmetrical plane horizontally intersecting the cylinder, the focal area and the focal volume are given as $\pi\omega^2$ and $2\pi\omega^2 d_z$, respectively, when the interface is observed. The depth profile has ∼10 μm of the full width at half-maximum (fwhm), corresponding to $d_z = \sim 5$ μm (see Figure 2). In the present confocal configuration, the focal volume turns out to have ∼10 μm in depth and ∼0.4 μm in radius, and hence becomes $\sim 5 \times 10^{-15}$ L.

Results

Fluorescence of DCM-Labeled *n*-Decane Droplets. An emulsion consisting of DCM-labeled *n*-decane droplets with the average diameter of ∼2000 nm dispersed in water was placed on a cover slip, and spike-like fluorescence signals with a given wavelength (537−673 nm) were measured. Figure 3 shows the time evolutions of the spike-like signals at different fluorescence wavelengths. Each spike-like fluorescence signal is attributed to one *n*-decane droplet containing fluorescing DCM molecules passing through the focal volume. Fluorescence signals from droplets with diameters smaller than 200 nm were found to be out of the detection limit in the present experimental setup. An averaged spike height at a given fluorescence wavelength was obtained by averaging the heights of spike trains collected for 104 s. The average spike height thus obtained is plotted against the fluorescence wavelength as shown in Figure 4; the spectra for the droplets with the average diameters of 300 ± 100 (●) and 2000 ± 1000 nm (○) have the maxima at the wavelengths of ∼640 and ∼625 nm, respectively. The droplets with diameters of 300 and 2000 nm were chosen for the spectral measurement, because they are stable in a time much longer than the measurement time. Although the droplets with a diameter of 50 nm are also stable, we disregarded the measurement of its spectrum because the detection system is not sensitive enough.

Fluorescence of DCM in the Flat *n*-Decane−Water Interface. Figure 5 shows the fluorescence spectra of a DCM-containing *n*-decane−water flat interface, when the focal region of the fluorescence microscope is located in the *n*-decane liquid

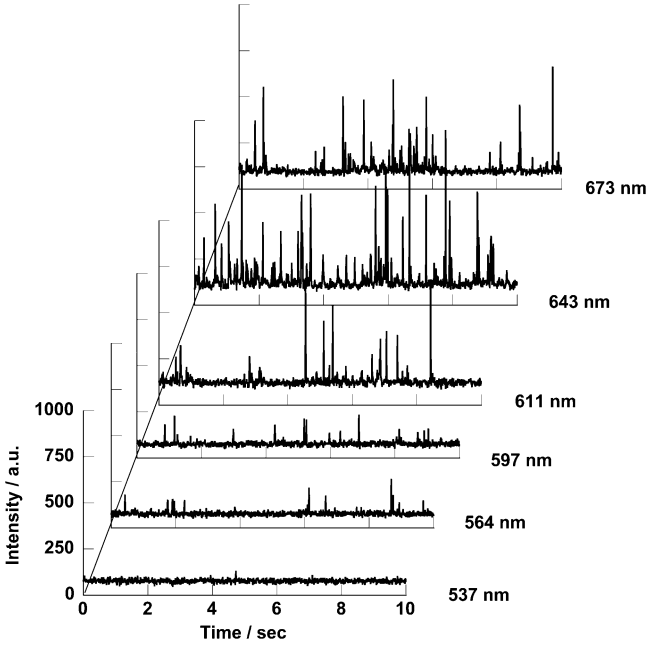

Figure 3. Signals of DCM fluorescence monitored at different wavelengths. DCM-labeled *n*-decane droplets with diameters of ∼2000 nm are dispersed in water. Each spike signal corresponds to one *n*-decane droplet passing through the focal region of the confocal fluorescence microscope.

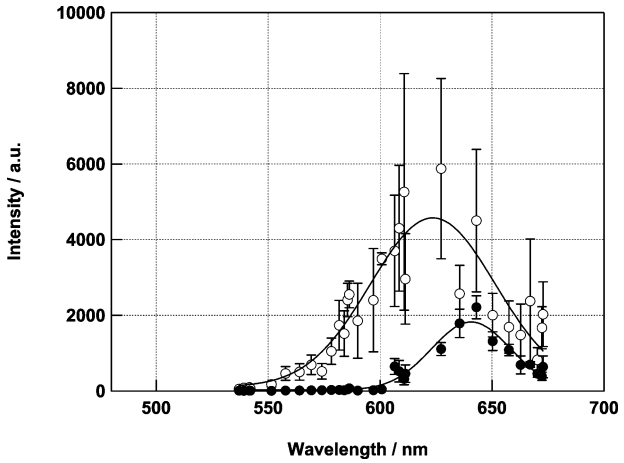

Figure 4. Fluorescence spectra of DCM in *n*-decane droplets with a diameter of ∼2000 (○) and ∼300 nm (●). The solid line shows Gaussian fitting of the experimental points.

(panel a), the interface between the *n*-decane and the water (panel b), and the water (panel c), respectively. As shown in Figure 5, the spectrum obtained at the *n*-decane liquid shows the peak in the region of 500−600 nm (see the spectrum measured by the fluorescence spectrometer given in the inset of panel a), while that at the interface does the peak at ∼625 nm. No signal is obtained (see panel c) when the probe is in the water, because of an extremely low solubility of DCM in water. Note that a single molecule detection is not achieved in these measurements, probably because the probe volume is not sufficiently small to detect a single molecule in this experimental condition.

Figure 6 shows the intensity of fluorescence at the wavelength of 625 nm probed at a focal region that is located in the flat interface as a function of the DCM concentration. The intensity of the 625-nm fluorescence from the interface increases, while those from the *n*-decane liquid and the water remain unchanged as the DCM concentration increases.

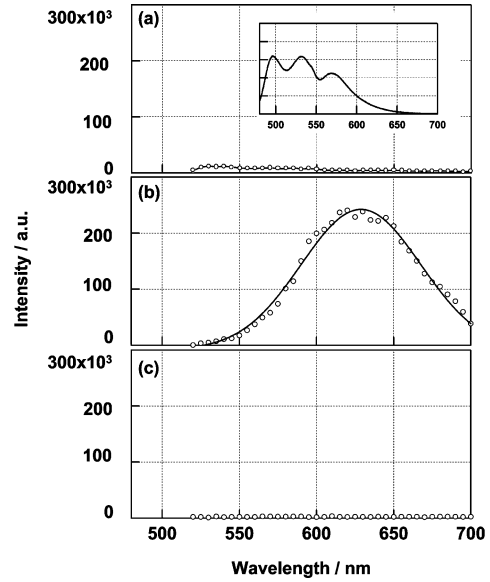

Figure 5. Fluorescence spectra of DCM in *n*-decane (a), in *n*-decane−water interface (b), and in water (c). The inset in panel a shows the spectrum of DCM in *n*-decane measured by a fluorescence spectrometer.

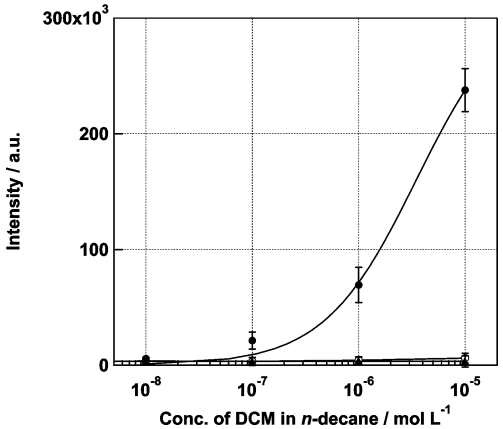

Figure 6. Fluorescence intensity of DCM in a *n*-decane (○) liquid, in a *n*-decane−water interface (●), and in water (▲) as a function of the DCM concentration; the fluorescence was monitored at a wavelength of 625 nm. The solid line for the closed circles represents the fitting curve calculated from the eq 4.

Discussion

Selective Fluorescence of DCM Molecules in the Surface Region of *n*-Decane Droplets. Figure 4 shows the fluorescence spectra of DCM molecules in *n*-decane droplets with an average diameter of ∼300 (●) and ∼2000 nm (○) in water, which exhibit peaks at ∼640 and ∼625 nm, respectively. It is concluded, as argued below, that the fluorescence originates from DCM molecules present in the surfaces of the droplets, which provide a polar environment to the DCM molecules. It is obvious that the DCM molecules are confined in the *n*-decane droplets because they are totally insoluble in the water. DCM molecules in the hydrophobic cores of the droplets fluoresce in the wavelength range centering at ∼530 nm, because the cores are nonpolar; as stated in the previous section, DCM molecules in a nonpolar environment emit fluorescence in the vicinity of ∼530 nm. As argued in the following sections, the number density of DCM molecules in the cores of the droplets is negligibly small, when the quantum efficiency (∼0.01) and the fluorescence intensity at ∼530 nm are taken into account.[28,29] On the other hand, DCM molecules in the surface region of the droplets are exposed partly to a polar atmosphere of water, and hence should emit fluorescence in the vicinity of ∼625 nm because DCM molecules in a polar environment fluoresce with a quantum efficiency of ∼0.4 in the wavelength region of ∼620 nm.[19−24]

DCM molecules in the core of a *n*-decane droplet can be probed selectively by observing fluorescence at the wavelength of ∼530 nm, while those in the peripheral region of the droplet surface in touch with liquid water can be probed by observing fluorescence at the wavelength of ∼625 nm, because DCM molecules in the core emit fluorescence centering at the wavelength of 530 nm and those in the peripheral region emit fluorescence centering at the wavelength of 625 nm. The selective detection of DCM molecules in the core and the peripheral region can be achieved satisfactorily if DCM molecules in the core do not emit any fluorescence in the wavelengths at ∼625 nm and those in the peripheral region do not in the wavelengths at ∼530 nm. If any, these undesired fluorescence signals give rise to a systematic error in determining the number density of DCM molecules. Let us estimate the contribution of the undesired signals; as described above, the fluorescence of DCM molecules in the core could have a contribution at the wavelengths of ∼625 nm, and the fluorescence of DCM molecules in the peripheral region could have a contribution at the wavelengths of ∼530 nm. To this end, we prepared a *n*-decane liquid containing 10^{-5} mol L^{-1} of DCM in contact with liquid water. Then, the fluorescence spectra were measured by placing the focal region of the confocal fluorescence microscope in the *n*-decane liquid and in the flat interface between the two liquids. As shown in Figures 5 and 6, the fractions of the undesired fluorescence signals are 0.3 and 0.02 for the detection of DCM molecules in the core (530-nm fluorescence) and the peripheral region (625-nm fluorescence), respectively. It is concluded that the number density of DCM molecules in the core of a *n*-decane droplet can be determined by using the 530-nm fluorescence detector with a systematic error of ∼30%, while that in the peripheral region of the droplet surfaces is determined with a systematic error of ∼2%.

Distribution of DCM Molecules in the *n*-Decane Droplet. The ratio, R_n, of the number density of DCM molecules in the surface region of a droplet to that in the core of a *n*-decane droplet dispersed in water is given by

$$R_n = \frac{A_d N_s^*}{V_d C_o^*} \tag{1}$$

where V_d and A_d represent the volume and the surface area of the *n*-decane droplet, respectively, and N_s^* and C_o^* represent the number density of the DCM molecules in the surface region of the droplet and that in the core of the droplet, respectively. For simplicity, we assume that the ratio N_s^*/C_o^* is independent of the curvature of the interface, that is, N_s^*/C_o^* is approximated by the corresponding ratio N_s/C_o for the flat interface between *n*-decane and the water liquids. For the flat interface, the ratio N_s/C_o is given by

$$\frac{N_s}{C_o} = \frac{I_s V_f \eta_o \epsilon_o}{I_o A_f \eta_s \epsilon_s} \tag{2}$$

where I_s and I_o show the 625- and 530-nm fluorescence intensities, and η and ϵ represent the quantum efficiency and the absorption coefficient, respectively. The subscripts s and o exhibit DCM in the interface and in the *n*-decane, respectively. The ratios η_s/η_o and ϵ_s/ϵ_o are approximated to be 40 and 10,

respectively. The spectral feature of DCM in methanol resembles that in the peripheral region of the *n*-decane−water interface, while the spectral feature of DCM in *n*-heptane does that in *n*-decane. In addition, the quantum efficiency of DCM at a *n*-decane−water interface is assumed to be ∼0.4, because DCM molecules in the Stern layer (polar environment) of micelles in anionic (sodium dodecyl sulfate (SDS), etc.) and cationic (cethyl trimethylammonium bromide (CTAB), etc.) micelle solutions fluoresce at a wavelength of ∼620 nm with a quantum efficiency of ∼0.35 and ∼0.40, respectively.[28] By taking these facts into consideration, the η_s and ϵ_s values are approximated by those of DCM molecules in the Stern layer of micelles[28] or methanol,[19−24] while the η_o and ϵ_o values are approximated by those of DCM molecules in *n*-heptane.[28,29] The ratios, R_n, of the number density of DCM molecules in the surface region of the droplet to that in the core of a *n*-decane droplet were led to be over ∼0.99 for 2000- and 300-nm droplets, respectively. Namely, most of the DCM molecules in a *n*-decane droplet are preferred to be present in the surface region of the droplet. This conclusion is consistent with the fluorescence spectra of DCM molecules in the droplets, in which no discernible peak is present in the vicinity of ∼550 nm ascribable to DCM molecules in *n*-decane.

Adsorption Isotherm of DCM on the *n*-Decane−Water Flat Interface. Let us consider "adsorption" of DCM molecules in the flat interface between *n*-decane and water liquids. The confocal microscope is set so that the focal volume crosses at the interface with an area A_f. If self-quenching and energy transfer between the adsorbed DCM molecules are disregarded, the fluorescence intensity, I_F, of the adsorbed DCM molecules is proportional to the number density, N_s, of DCM molecules in the focal area, and is given as

$$I_F = GN_sA_f \tag{3}$$

where *G* is a constant; in the present experimental condition, *G* turns out to be the number of photon counts detected per DCM molecule in 13 s. The adsorption isotherm of the DCM molecules on the flat interface was obtained through measuring the fluorescence intensities of DCM in the interface and inside the *n*-decane liquid as a function of the DCM concentration in the *n*-decane liquid (see Figure 6). We employed the Langmuir adsorption isotherm for describing the condensation of DCM molecules in the peripheral region of the interface, since it is successfully applied to various systems akin to the present system such as adsorption of neutral hydrophobic molecules in air−liquid,[30] solid−liquid,[31] and liquid−liquid[16] interfaces. The number density, N_s, of the DCM molecules in the interface is expressed by the Langmuir adsorption isotherm as

$$N_s = \frac{N_{max}KC_o}{1 + KC_o} \tag{4}$$

where N_{max} is the number density of the DCM molecules at saturation, and *K* is the equilibrium constant of adsorption (Langmuir constant). By fitting the fluorescence intensity (I_F) vs the concentration (C_o) relationship to the Langmuir adsorption isotherm (eq 4), the values of *K* and GN_{max} were obtained to be $(2.9 \pm 0.3) \times 10^5$ M^{-1} and $(2.5 \pm 0.08) \times 10^4$ counts/s, respectively. The Gibbs energy of adsorption, $-\Delta G_{ads}^\circ$, corresponding to the adsorption constant *K*, was further calculated to be 30 ± 1 kJ mol^{-1} with the relation $\Delta G_{ads}^\circ = -RT \ln K$, where *R* is the gas constant and *T* is the absolute temperature (296 K).[8,16] As for adsorption of dioctadecyl-rhodamine B dissolving in cyclohexane on a cyclohexane−water interface, the Gibbs energy of adsorption, $-G_{ads}^\circ$, which is obtained by using the Langmuir adsorption isotherm, is reported to be 39 kJ mol^{-1},[16] which is comparable to the adsorption energy of amphiphiles being adsorbed from an organic phase on a liquid−liquid interface.[32] The dioctadecyl-rhodamine B molecules at the interface are in the zwitterionic and cationic forms,[33] rather than in the lactone form.

Solvation of the Surface Region of *n*-Decane Droplets. DCM molecules in *n*-decane droplets having an average diameter of ∼300 and ∼2000 nm emit fluorescence peaked at ∼640 and ∼625 nm, respectively (see Figure 4). This peak shift due to the change of the droplet diameter indicates that DCM molecules in the surface region of a 300-nm droplet feel a more polar environment than those in the surface region of a 2000-nm droplet do. Namely, the polarity of the surface region of a droplet changes with its diameter. If solvent (or environment) relaxation is complete, an equation for a solvatochromic shift due to a dipole−dipole interaction can be derived on the basis of a simple model of spherical-centered dipoles in isotropically polarizable spheres on the assumption of equal dipole moments in Franck−Condon and relaxed states.[34]

Let us consider that DCM molecules in a solvent absorb photons at the wavelength of ν_a, at which the absorbance reaches the maximum and fluoresce at the wavelength of ν_f, at which the fluorescence intensity reaches the maximum. The difference, $\nu_f - \nu_a$, is expressed in terms of the polarizability felt by the DCM molecules. As described previously, almost all the DCM molecules are in the vicinity of the droplet surface, at which the DCM molecules fluoresce via the twisted intramolecular charge transfer (TICT) state. It has been shown that the shift of the absorption peak is much smaller than that of the fluorescence peak when the TICT state is involved. Under these circumstances, the following relation holds:[25−27]

$$\nu_f = -A\Delta f + C \tag{5}$$

with

$$\Delta f = \frac{\epsilon - 1}{\epsilon + 2} - \frac{n^2 - 1}{2n^2 + 4} \tag{6}$$

where *A* is a coefficient related to the polarizability of a DCM molecule, Δf is the orientation polarizability, ϵ and *n* are the dielectric constant and the refraction index, respectively, and *C* is a constant. The *A* and *C* values in eq 5 were determined to be 18.9×10^3 (cm^{-1}) and 3.52×10^3 (cm^{-1}), respectively, by using the absorption and the fluorescence spectra of DCM dissolved in various solvents having $0.09 < \Delta f < 0.81$ (see Figure 7).

By taking advantage of eq 5, the orientation polarizability (Δf) for 300- and 2000-nm droplets turn out to be 0.94 and 0.84, respectively. It implies that DCM molecules in the surface region of a nonpolar *n*-decane droplet feel a strong polar environment; the field strength increases with decreasing the diameter of the droplet. This strong polar environment in the surface region of the droplet in touch with water molecules is likely to originate from hydrophobic hydration surrounding the nonpolar *n*-decane.[35,36] It is not plausible that the extent of the hydration changes with the droplet diameter in the range of several hundred nanometers, because the curvature of the droplet in these diameters is much smaller than the dimension of water molecules. It is more likely that the strongly interacted hydrogen-bonding network of water molecules in the surface region of a droplet is closely related to the OH^- ions present in the droplet surface. A number of OH^- ions adhere on the surface of the

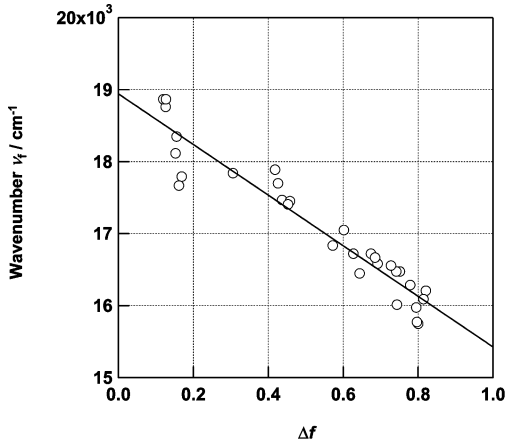

Figure 7. Lippert's plot for various solvents by using Table 1 in ref 27; orientation polarizability, Δf, vs the wavenumber, ν_f, of the fluorescence.

droplets and interfacial water molecules are tightly bound to OH^-. The surface potential at the oil−water interface is known to originate from a strong dipole moment or the hydrogen bonding of the OH^- ions with the hydrogen atoms of the interfacial water molecules.[37−39] Indeed, the surfactant-free *n*-decane droplets have a negative surface potential (ζ-potential) and the potential increases with a decrease in the droplet size.[18] Namely, the number of OH^- ions interacting with the hydrogen atoms of the interfacial water molecules per unit surface area increases with a decrease in the droplet size. A tighter hydrogen-bonding network must be formed around smaller droplets because of a higher density of OH^- ions. In the present fluorescence spectroscopy of DCM in *n*-decane droplets, the red shift of maximum wavelength of DCM in the surface region of smaller droplets suggests that a tighter hydrogen-bonding network must be formed around smaller droplets.

Summary

By use of confocal fluorescence microscopy, we investigated the fundamental properties of a curved interface between a DCM-labeled *n*-decane droplet and liquid water and a flat interface between bulk DCM-labeled *n*-decane and water. In particular, it is revealed that the surface of the *n*-decane droplet is polarized and its polarity increases with increasing the curvature or decreasing the droplet diameter. The present study shows that this methodology provides key information on the polarity of the peripheral region of the curved liquid interfaces, and demonstrates the utility of this methodology for the investigation of a curved liquid interface as well as a flat liquid interface.

Acknowledgment. The authors are indebted to Professor R. N. Zare and Professor D. T. Chiu for technical advice for the single molecule detection method. This work was supported by the Cluster Research Project of the Genesis Research Institute, Inc.

References and Notes

(1) Corn, R. M.; Higgins, D. A. *Chem. Rev.* **1994**, *94*, 107.
(2) Naujok, R. R.; Paul, H. J.; Corn, R. M. *J. Phys. Chem. A* **1996**, *100*, 10497.
(3) Messmer, M. C.; Conboy, J. C.; Richmond, G. L. *J. Am. Chem. Soc.* **1995**, *117*, 8039.
(4) Miranda, P. B.; Shen, Y. R. *J. Phys. Chem. B* **1999**, *103*, 3293.
(5) Watarai, H.; Funaki, F. *Langmuir* **1996**, *12*, 6717.
(6) Piasecki, D. A.; Wirth, M. J. *J. Phys. Chem.* **1993**, *97*, 7700.
(7) Zhang, Z. H.; Tsuyumoto, I.; Kitamori, T.; Sawada, T. *J. Phys. Chem. B* **1998**, *102*, 10284.
(8) Zhang, Z. H.; Tsuyumoto, I.; Takahashi, S.; Kitamori, T.; Sawada, T. *J. Phys. Chem. A* **1997**, *101*, 4163.
(9) Eigen, M.; Rigler, R. *Proc. Natl. Acad. Sci. U.S.A.* **1994**, *91*, 5740.
(10) Nie, S.; Chiu, D. T.; Zare, R. N. *Anal. Chem.* **1995**, *67*, 2849.
(11) Schmidt, T.; Schutz, G. J.; Baumgartner, W.; Gruber, H. J.; Schindler, H. *J. Phys. Chem.* **1995**, *99*, 17662.
(12) Ambrose, W. P.; Goodwin, P. M.; Jett, J. H.; Orden, A. V.; Werner, J. H.; Keller, R. A. *Chem. Rev.* **1999**, *99*, 2929.
(13) Li, Y.-Q.; Sasaki, S.; Unoue, T.; Ogawa, T. *Laser Chem.* **1998**, *17*, 175.
(14) Zheng, X.-Y.; Harata, A.; Ogawa, T. *Chem. Phys. Lett.* **2000**, *316*, 6.
(15) Zheng, X.-Y.; Harata, A.; Ogawa, T. *Spectrochim. Acta*: *Part A* **2001**, *57* (2), 315.
(16) Zheng, X.-Y.; Harata, A. *Anal. Sci. J.* **2001**, *17*, 131.
(17) Sakai, T.; Takeda, Y.; Mafuné, F.; Abe, M.; Kondow, T. *J. Phys. Chem. B* **2002**, *106* (19), 5017.
(18) Sakai, T.; Takeda, Y.; Mafuné, F.; Abe, M.; Kondow, T. *J. Phys. Chem. B* **2003**, *107* (13), 2921.
(19) Gustavsson, T.; Baldacchino, G.; Mialocq, J.-C.; Pommeret, S. *Chem. Phys. Lett.* **1995**, *236*, 587.
(20) van der Meulen, P.; Zhang, H.; Jonkman, A. M.; Glasbeek, M. *J. Phys. Chem.* **1996**, *100*, 5367.
(21) Zhang, H.; Jonkmann, A. M.; van der Meulen, P.; Glasbeek, M. *Chem. Phys. Lett.* **1994**, *224*, 551.
(22) Easter, D. C.; Baronavski, A. P. *Chem. Phys. Lett.* **1993**, *201*, 153.
(23) Rettig, W.; Majenz, W. *Chem. Phys. Lett.* **1989**, *154*, 335.
(24) Gilabert, E.; Lapouyade, R.; Rulliere, C. *Chem. Phys. Lett.* **1988**, *145*, 262.
(25) Lippert, E. *Z. Naturforsch.* **1955**, *10a*, 541. Lippert, E. *Z. Elektrochem.* **1957**, *61*, 962.
(26) Mataga, N.; Kaifu, Y.; Koizumi, M. *Bull. Chem. Soc. Jpn.* **1956**, *29*, 465.
(27) Mayer, M.; Mialocq, J.-C. *Opt. Commun.* **1987**, *64*, 264.
(28) Pal, S. K.; Sukul, D.; Mandal, D.; Sen, S.; Bhattacharyya, K. *Chem. Phys. Lett.* **2000**, *327*, 91.
(29) Pal, S. K.; Mandal, D.; Sukul, D.; Bhattacharyya, K. *Chem. Phys. Lett.* **1999**, *312*, 178.
(30) Castro, A.; Bhattacharyya, K.; Eisenthal, K. B. *J. Chem. Phys.* **1991**, *95* (2), 1310.
(31) Hansen, R. L.; Harris, J. M. *Anal. Chem.* **1998**, *70*, 2565.
(32) Higgins, D. A.; Corn, R. M. *J. Phys. Chem.* **1993**, *97*, 487.
(33) Arbeloa, I. L.; Rohatgi-Mukherjee, K. K. *Chem. Phys. Lett.* **1986**, *128*, 474.
(34) Valeur, B. *Molecular Fluorescence*; Wiley-VCH: New York, 2001.
(35) Sharp, K. A.; Nicholls, A.; Fine, R. F.; Honig, B. *Science* **1991**, *25*, 106.
(36) Southall, N. T.; Dill, K. A. *J. Phys. Chem. B* **2000**, *104* (6), 1326.
(37) Taylor, A. J.; Wood, F. W. *Trans. Faraday Soc.* **1957**, *53*, 523.
(38) Marinova, K. G.; Alargova, R. G.; Denkov, N. D.; Velev, O. D.; Petsev, D. N.; Ivanov, I. B.; Borwankar, R. P. *Langmuir* **1996**, *12*, 2045.
(39) Stachurski, J.; Michalek, M. *J. Colloid Interface Sci.* **1996**, *184*, 433.